Postmortem evidence of microglial involvement in the child abuse-associated increase of perineuronal nets in the ventromedial prefrontal cortex

Running title: Early-life stress and human microglia

Claudia Belliveau[1,2,†], Reza Rahimian[1,†], Gohar Fakhfouri[3], Maria Antonietta Davoli[1], Bruno Giros[2,3], Gustavo Turecki[1,2,3] and Naguib Mechawar[1,2,3]

(†) shared first authorship

Affiliations

[1]McGill Group for Suicide Studies, Douglas Mental Health University Institute, McGill University, Montreal, Qc, Canada

[2] Integrated Program in Neuroscience, McGill University, Montreal, Qc, Canada

[3] Department of Psychiatry, McGill University, Montreal, Qc, Canada.

Acknowledgments

We are deeply indebted to the next of kin who consented to donating the brains of their loved ones.

Word Count: 5473

Keywords: Humans, Mice, Adverse Childhood Experiences, Microglia, Extracellular Matrix, Matrix Metalloproteinase 9

Corresponding Author

Naguib Mechawar, PhD

Douglas Mental Health University Institute

Department of Psychiatry, McGill University

naguib.mechawar@mcgill.ca

Table of Contents Main Points:

- Microglia are increasingly recognized for their involvement in regulating a specialized form of extracellular matrix known as perineuronal nets.
- Perineuronal net densities are increased in the ventromedial prefrontal cortex of depressed suicides with a history of child abuse.
- Microglia secrete less matrix metalloproteinases that are responsible for the degradation of perineuronal nets, specifically microglial MMP-9.
- Intercellular communication between microglia and neurons through IL33R and CX3CR1 is also dampened.

Table of Contents Image:

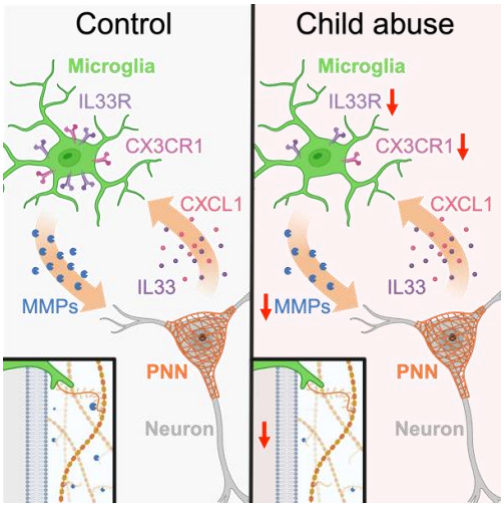

Abstract

Microglia, versatile in their functions within the central nervous system, have recently been recognized for their capacity to degrade extracellular matrix. Perineuronal nets (PNNs), a specialized form of this matrix, are crucial for stabilizing neuronal connections and constraining plasticity. Our group recently reported increased PNN densities in the ventromedial prefrontal cortex (vmPFC) of adult depressed suicides with a history of child abuse, compared to matched controls. To explore the underlying mechanisms, we used here a comprehensive approach in similar postmortem vmPFC samples, combining a human matrix metalloproteinase array, isolation of CD11b-positive microglia and enzyme-linked immunosorbent assays. Our results indicate a significant downregulation of matrix metalloproteinase (MMP)-9 and tissue inhibitors of metalloproteinases (TIMP)-2 in both whole vmPFC grey matter and isolated microglia. Furthermore, our experiments revealed that a history of child abuse was associated with a dampening of intercellular communication between microglia and neurons through CX3CR1 and IL33R. Taken together, these findings suggest that microglial function is lastingly disrupted in the vmPFC of adults having experienced sever adversity during childhood, thus providing a potential mechanism for the previously reported child abuse-associated PNN alterations.

Introduction

Microglia, the brain's resident immune cells, play a fundamental role in the induction of neuroinflammation through their ability to transform into reactive states in response to inflammatory insults (Javanmehr et al., 2022; Wright-Jin & Gutmann, 2019). A large body of evidence has established that neuroinflammation may play an instrumental role in major depressive disorder (MDD) (B. Li et al., 2022; Rahimian et al., 2022; Rahimian et al., 2021; Troubat et al., 2021), at least in certain patients, through the chronic priming of microglia in limbic regions (Torres-Platas et al., 2014). Furthermore, microglia respond to environmental signals such as stress by releasing various molecules (cytokines, chemokines and growth factors) and by regulating phagocytosis and synaptic pruning, which are crucial for proper brain development and function (Schramm & Waisman, 2022). Microglia have also recently gained attention for their role in early-life stress (ELS) (Bolton et al., 2022; Catale et al., 2020; Reemst et al., 2022) and regulating brain plasticity through modulation of the extracellular matrix (ECM) (reviewed in (Crapser et al., 2021; Dzyubenko & Hermann, 2023)). One specialized form of condensed ECM, perineuronal nets (PNNs), function to inhibit axon growth and spine formation (Monnier et al., 2003; Pearson et al., 2018) while acting as a scaffolding for neuronal circuitry (Sigal et al., 2019; Tsien, 2013). Emerging evidence implicates microglia as key players in PNN degradation (Arreola et al., 2021; Crapser et al., 2021; Crapser, Ochaba, et al., 2020; Crapser, Spangenberg, et al., 2020; Nguyen et al., 2020; Sun et al., 2023; Venturino et al., 2021). The mechanisms underlying this phenomenon, however, remain incompletely understood. Instances of direct PNN regulation through microglial phagocytosis have been recognized, as evidenced by PNN staining (*Wisteria Floribunda Lectin* (WFL) or anti-aggrecan) visible in CD68+ lysosomes of microglia in healthy brain (Nguyen et al., 2020; Sun et al., 2023; Venturino et al., 2021) and spinal cord (Tansley et al.,

2022), Alzheimer's Disease (Crapser, Spangenberg, et al., 2020), Huntington's Disease (Crapser, Ochaba, et al., 2020) and adult-onset leukoencephalopathy with axonal spheroids and pigmented glia (Arreola et al., 2021) brains. The existing body of literature underscores the significance of intercellular communication between neurons and microglia in the intricate regulation of PNNs. However, it remains uncertain whether these communication pathways are fully responsible for initiating microglial phagocytosis of PNN components or if they just represent one mechanism. The interaction between neuronal IL33 and microglial IL33-receptor (IL33R) is a good example. This interaction has been shown to trigger microglial phagocytosis of PNN component aggrecan; an effect abolished in knockout mice of either the ligand or receptor (Nguyen et al., 2020). PNN phagocytosis similarly occurs with neuronal CX3CL1 binding to microglial CX3CR1, as demonstrated by reduced PNN density in parallel to WFL accumulation in CD68+ microglial lysosomes. Knocking out either CX3CL1 or CX3CR1 also prevents this from occurring (Tansley et al., 2022).

Matrix metalloproteinases (MMPs) are enzymes that catalyze glycoproteins in the ECM. Their activity is tightly controlled in the healthy brain by endogenous tissue inhibitors (TIMP-1, -2, -3, -4) that bind to their catalytic site (Laronha & Caldeira, 2020). MMPs can be classified, based on their affinity to various substrates, into different subgroups: gelatinases (MMP-2, -9), stromelysins (MMP-3, -10 and -11) and collagenases (MMP-1, -8, -13, -18) among others (Laronha & Caldeira, 2020). Importantly, all classes of MMPs have already been implicated in ECM regulation. Specifically, they have all been found to target aggrecan core protein, tenascins and link proteins which are all fundamental components of PNNs (Könnecke & Bechmann, 2013; Laronha & Caldeira, 2020). Different types of MMPs, especially MMP-2 and MMP-9, are expressed by

microglia and their roles have been established in neuroinflammatory cascades (Könnecke & Bechmann, 2013). The most studied MMP, MMP-9, plays a fundamental role in neurodevelopment (myelination and synaptic pruning) and homeostasis in adulthood (Bitanihirwe & Woo, 2020). Studies show that MMP-9, released by glia and neurons, is directly responsible for pruning PNNs, as shown by increased densities of PNNs following genetic deletion of the MMP-9 gene (Wen et al., 2017). Interestingly, antidepressant efficacy in stressed mice has also been linked to PNN degradation by MMP-9 (Alaiyed et al., 2019).

In a recent postmortem study, we identified in depressed suicides a child abuse-associated increase in WFL+ PNNs in the lower layers of the ventromedial prefrontal cortex (vmPFC) (Tanti et al., 2022) a cortical region critically involved in decision-making, impulsivity and suicidal tendencies (Hiser & Koenigs, 2018; Teicher et al., 2016). The current study sought to explore the impact of child abuse on the regulation of PNNs by microglia in the same brain region. An unbiased MMP antibody array was used to quantify the relative expression of different MMPs in vmPFC using both grey matter lysate and in CD11b-positive ($CD11b^+$) isolated microglia. Additionally, canonical microglial markers implicated in ECM modulation such as CD68, CX3CR1, TREM2, IL33R and Cathepsin-S were quantified using enzyme-linked immunosorbent assay (ELISA). This multifaceted approach aimed at assessing comprehensively the intricate molecular mechanisms underlying the influence of early-life adversity on PNNs in the vmPFC.

Methods

Human brain samples

The postmortem human brain samples used in this study were provided by the Douglas-Bell Canada Brain Bank (DBCBB) (Montreal, Canada) with ethical approval from the Douglas Research Ethics Board (IUSMD-20-35). Brains, donated by familial consent, were acquired by the DBCBB thanks to a collaboration between the McGill Group for Suicide Studies and the Quebec Coroner's Office. A panel of psychiatrists created clinical vignettes for each individual by compiling all available information obtained from medical records, the coroner's report, toxicological analyses, and other sources of information, as described previously (A. Dumais et al., 2005). Samples used in this study were from psychiatrically healthy controls (CTRL) and depressed suicides with a history of severe child abuse (DS-CA). Non-random childhood abuse (sexual, physical and neglect) was assessed through a standardized psychological autopsy with next of kin, using a modified version of the Childhood Experience of Care and Abuse (CECA) (Bifulco et al., 1994). Only the most severe cases (score of 1-2) occurring before the age of 15 were included in the DS-CA group. Any indication of neurodevelopmental, neurological, or other co-morbid mental illnesses were cause for exclusion.

Brains were cut into 0.5cm-thick coronal sections upon arrival at the DBCBB then flash-frozen in isopentane at -35°C and stored at -80°C until use, referred to hereafter as archived frozen brain samples. Expert staff at the DBCBB dissected vmPFC (Brodmann area 11/12) at the equivalent of plate 3 (approximately -48 mm from the center of the anterior commissure) of the Mai and Paxinos Atlas of the Human Brain (Juergen Mai, 2016). Group characteristics of archived frozen brain samples are outlined in **Table 1**.

Human MMP Antibody Array

Grey matter was dissected from archived frozen vmPFC samples and lysed using RIPA buffer (Sigma, St. Louis, MO, USA) and then protein concentration was measured on a TECAN microplate reader. A human MMP antibody array (RayBiotech® C-Series, Human MMP Array C1, Norcross, GA, USA) was used to compare the relative abundance of 10 MMPs and their inhibitors (TIMPs) between CTRL and DS-CA samples according to the manufacturer's protocol. This array allows for the semi-quantitative analysis of MMP-1, -2, -3, -8, -9, -10 and -13 as well as of TIMP-1, -2 and -4. Unfortunately, MMP-10 was removed from the analyses because quantities were too low and outside of the quantifiable range. An antibody array membrane was used per subject, each processed in separate wells of the provided incubation tray, printed side up. Membranes were incubated under constant agitation for 30 mins at room temperature (RT) with 2 ml of blocking buffer. Next, 1 ml of diluted sample containing 150μg of protein was added to each well and incubated overnight at 4°C under constant agitation. Membranes were washed for 5 minutes at RT thrice with Wash Buffer 1 and twice with Wash Buffer 2. Membranes were then incubated with 1 ml of the prepared Biotinylated Antibody Cocktail and incubated overnight at 4°C under constant agitation. Wash Buffer 1 + 2 were used as described above. Membranes were incubated for 2h at RT with 1X HRP-Streptavidin followed by Wash Buffer 1 + 2. Lastly, chemiluminescence detection was completed using the Detection Buffers provided. 2-D densitometry was conducted using ImageJ to detect the spot signal densities. Relative expression was calculated by subtracting background from each spot and normalizing to a reference positive control spot. Each antibody was spotted in duplicate on the membrane so normalized relative expression was averaged per subject to obtain a single measurement per antibody.

ELISA

ELISA was employed for quantitative measurement of human CD68 (cluster of differentiation 68), CX3CR1 (CX3C motif chemokine receptor 1), Cathepsin-S (Cat-S), TREM2 (triggering receptor expressed on myeloid cells 2), and IL33R (interleukin 33 receptor/ST2) in vmPFC samples following the manufacturer's instructions. In brief, grey matter was dissected from the archived frozen vmPFC and lysed using RIPA buffer (Sigma, St. Louis, MO, USA). Total protein concentration for each sample was measured using a BCA Protein Assay kit (cat # 23225, Thermo Fisher Scientific, Saint-Laurent, Quebec, Canada). Depending on the assay, 50-100 μg total protein and standards were added to antibody pre-coated wells and after addition of conjugated antibodies specific to the analyte of interest (sandwich ELISA) or conjugated-analyte in the case of CD68 (competitive ELISA) microplates were incubated at 37°C for 60 minutes. Substrate addition led to color development in proportion to the amount of the analyte, except for CD68 kit, where the intensity of the color (optical density, OD) was inversely proportional to the CD68 concentration. The reaction was terminated by addition of acidic stop solution and absorbance was read at 450 nm. A standard curve was plotted relating the OD to the concentration of standards. The analyte concentration (pg/ml or ng/ml) in each sample was then interpolated from the corresponding standard curve. Optimal sample protein amounts for each ELISA assay were determined in a pilot experiment to ensure OD values would fall within the range of the corresponding standard curve. A detailed description of the procedure is found on MyBioSource.com.

Western Blotting

The same samples were used for ELISA and Western Blotting. Pilot tests were conducted to find out whether chondroitinaseABC (chABC) digestion of the samples was necessary prior to

immunoblotting. We observed no discernible differences between samples subjected to various durations of chABC digestion (20h, 1h, 30mins) and those left untreated, and thus omitted this step to streamline the process and optimize time efficiency. 4-20% Mini-PROTEAN® TGX Stain-Free Protein, 12 well, 20 µl gels (cat # 4568095, Bio-Rad, Hercules, CA, USA) were used to separate proteins based on size. Blots were probed with an antibody for the N-terminal (DIPEN) neo-epitope of aggrecan core protein cleaved by MMP between amino acids PEN341 and 342FFG (clone BC-4, 1:100, cat # 1042002, MDBioproducts, Oakdale, MN, USA). Prior to gel loading, samples were prepared by adding 1X Laemmli Buffer and incubated at 95°C for 5 minutes, followed by centrifugation and subsequent placement on ice for 3 minutes. Equal volumes were loaded into the gradient gels (each sample 35 µg of protein) and electrophoresis was conducted for 50 minutes at 135 mV in a Bio-Rad Mini-PROTEAN® Tetra Cell electrophoresis chamber containing 1X running buffer, with constant agitation facilitated by a magnetic stir bar. Preceding the 30-minute semi-dry standard protein transfer from the gel to a nitrocellulose membrane, stain-free gels were activated for 45 seconds on a Chemi-doc to capture a total protein control image. Following a 1-hour blocking step in 5% milk in PBS-tween, the primary antibody, also diluted in the same solution, was incubated with the blot overnight at 4°C under continuous agitation. Post-incubation, three 10-minute washes in PBS-Tween were performed, and a secondary Amersham ECL sheep anti-mouse, horseradish peroxidase linked IgG antibody (1:1000, cat # NA931, Cytvia, Marlborough, MA, USA) was subsequently incubated in 1% milk in PBS-tween for 2 hours at room temperature, again under constant agitation. Blots were subjected to three additional 10-minute washes in PBS-Tween before being exposed to an enhanced chemiluminescence (ECL) solution (1:1) for 1 minute. The blots were imaged on the Chemi-doc system using predefined settings.

Subsequent blot analyses adhered to the guidelines provided by Bio-Rad. Each blot incorporated a reference lane comprising a composite of all samples, serving as an inter-gel control. To succinctly outline the quantification process, the adjusted volume of the 50 kDa band was used to determine the protein mean intensity on the blot, while the adjusted volume for the entire lane on the stain-free gel provided a measure of total protein. Normalization of each sample was achieved by establishing a normalization factor, computed as the ratio of the total protein content of the sample to the adjusted volume of its corresponding stain-free gel. Subsequently, this factor was divided by the corresponding value for the reference lane, yielding a fold-difference. The resultant fold-differences were then compared between the CTRL and DS-CA.

CD11b$^+$ microglia isolation using magnetic beads

To measure the relative expression of different MMPs in vmPFC microglia, fresh brain tissue was acquired on a rolling basis from the DBCBB from December 2019 – July 2023. Upon arrival at the DBCBB, samples underwent immediate processing for CD11b+ microglia isolation, followed by MMP antibody array analysis, according to the following procedure. Miltenyi Biotec CD11b MicroBeads (cat # 130-093-634, Gaithersburg, MD, USA) were first used to isolate microglia. These beads were developed for the isolation or depletion of human and mouse cells based on their CD11b expression. In humans, CD11b is strongly expressed on myeloid cells such as cerebral microglia and weakly expressed on NK cells and some activated lymphocytes. Using a 1 cm^3 block of fresh-non-frozen vmPFC, grey matter was dissected and CD11b$^+$ microglia were isolated using a combination of enzymatic and mechanical dissociations following Miltenyi Biotec instructions. The Neural Tissue Dissociation Kit (Papain, cat # 130-092-628, Miltenyi Biotec, Gaithersburg,

MD, USA) and the gentleMACS™ Dissociator (cat # 130-093-235, Miltenyi Biotec, Gaithersburg, MD, USA) are effective in generating single-cell suspensions from neural tissues prior to subsequent applications, such as MACS® Cell Separation. After mechanical and enzymatic dissociation, red blood cells were eliminated using Red Blood Cell Lysis Solution (cat # 130-094-183, Miltenyi Biotec, Gaithersburg, MD, USA). These steps were followed by application of Debris Removal Solution, which is a ready-to-use density gradient reagent (cat # 130-109-398, Miltenyi Biotec, Gaithersburg, MD, USA), allowing for a fast and effective removal of cell debris from viable cells after dissociation of various tissue types, while applying full acceleration and full brake during centrifugation. Prior to the positive selection of $CD11b^+$ cells, Myelin Removal Beads were employed for the specific removal of myelin debris from single-cell suspensions (cat # 130-096-433, Miltenyi Biotec, Gaithersburg, MD, USA). Then, the $CD11b^+$ cells were magnetically labeled with CD11b MicroBeads and the cell suspension was loaded onto a MACS® Column, which was placed in the magnetic field of a MACS Separator. The magnetically labeled $CD11b^+$ cells were retained on the column, while the unlabeled cell fraction, which was depleted of $CD11b^+$ cells ran through the column. The magnetically retained $CD11b^+$ cells were finally eluted following removal of the column from the magnetic field. Lastly, the $CD11b^+$ cells were processed for Human MMP antibody array as described above. After rigorous characterization of the brain samples by psychological autopsy, as outlined previously, four subjects met inclusion criteria for DS-CA and could be matched to four healthy CTRL samples (**Table 2**).

Statistical analyses

Statistical analyses were conducted using GraphPad Prism v10.1.1 (Boston, MA, USA) and SPSS v 29.0 (IBM Corp, Armonk, New York, USA). We identified outliers utilizing Grubb's method

and assessed the distribution and homogeneity of variances through Shapiro–Wilk and Levene's tests, respectively. Independent samples t-tests were employed for all analyses with the exception being the comparison of time of death Cathepsin-S levels between groups where two-way analysis of variance (ANOVA) was applied (CTRL: n = 9, DS-CA: n = 14). Age showed no correlation with any of the presented results. pH exhibited correlations with IL33R and TREM2 levels, while the number of medications demonstrated correlations with whole grey-matter TIMP-2 levels. Additionally, the type of antidepressant and the number of medications were correlated with CX3CR1 levels (**Supplementary Table 1**). Postmortem interval (PMI) was significantly correlated with microglial MMP-2 and TIMP-2 levels (**Supplementary Table 2**). Consequently, a one-way analysis of covariance (ANCOVA) was applied, treating group as a fixed factor and pH, PMI or medications as a covariate for these variables. A two-tailed approach was used for all tests and p-values < 0.05 were considered significant. All data is presented as mean ± standard error of the mean unless otherwise specified.

Results

Downregulation of multiple MMPs in vmPFC grey matter of depressed suicides with a history of child abuse

A representative blot of the high-content screening human MMP antibody array used to assess the relative expression of MMPs and TIMPs in vmPFC grey matter is illustrated in **Fig. 1A**. This approach allowed us to measure a significant overall downregulation of MMPs in DS-CA compared to CTRLs. Notably, gelatinase MMP-9 exhibited a significant downregulation in DS-CA (P = 0.011) whereas MMP-2 was similar between groups (P = 0.43, **Fig. 1B**). Stromelysin MMP-3 was also significantly downregulated in DS-CA vs CTRL samples (P = 0.012, **Fig. 1C**),

as was collagenases MMP-1 (P = 0.036) and MMP-8 (P = 0.001, **Fig. 1D**). MMP-13 (P = 0.08) remained similar between groups (**Fig. 1D**). Interestingly, all three MMP inhibitors displayed significant downregulation in DS-CA: TIMP-1 (P = 0.005), TIMP-2 (F (1,19) = 28.14, P < 0.001) and TIMP-4 (P = 0.003, **Fig. 1E**).

Given the ubiquitous secretion of MMPs and TIMPs from nearly all cell types (Könnecke & Bechmann, 2013), we selectively isolated $CD11b^+$ microglia with CD11b magnetic beads from fresh brain samples and processed these cells for the MMP array. The measurement of MMPs and TIMPs in microglia are consistent with the results of a previous studies demonstrating the capacity of microglial translating mRNA to produce these enzymes (Boutej et al., 2017; Rahimian et al., 2024). In vmPFC microglia, gelatinase MMP-9 (P = 0.045) and inhibitor TIMP-2 (F(1,5) = 9.14, P = 0.029) displayed significant downregulation in DS-CA compared to CTRL. Meanwhile, MMP-2 (F(1,5) = 3.71, P = 0.11), Stromelysin MMP-3 (P = 0.050), all collagenases (MMP-1: P = 0.65, MMP-8: P = 0.27 and MMP-13: P = 0.73), TIMP-1 (P = 0.57) and TIMP-4 (P = 0.91) showed no significant difference between groups (**Fig. 2**). In sum, the concurrent downregulation of MMP-9 and TIMP-2 in both whole grey matter and isolated microglia suggested a dysregulation of microglial ECM degradation in DS-CA samples compared to matched controls.

Canonical microglial markers involved in the regulation of PNNs are dampened in DS-CA samples

We then conducted ELISAs to assess other molecules known to be involved in ECM modulation (Arreola et al., 2021; Crapser, Ochaba, et al., 2020; Crapser, Spangenberg, et al., 2020; Nguyen et al., 2020; Sun et al., 2023; Tansley et al., 2022; Venturino et al., 2021). CX3CR1 (F(1,19) = 45.49, P < 0.001, **Fig. 3A**) and IL33R (F(1,20) = 12.81, P = 0.0020, **Fig. 3B**) were both significantly

downregulated in DS-CA compared to CTRL vmPFC. Conversely, CD68 ($P = 0.30$, **Fig. 3C**), TREM2 ($F(1,20) = 0.14$, $P = 0.91$, **Fig. 3D**) and Cat-S ($P = 0.062$, **Fig. 3E**) levels were similar between groups. To account for the diurnal rhythm of Cat-S (Pantazopoulos et al., 2020), subjects were classified into two categories based on time of death (6:00AM to 5:59PM: Day; 6:00PM-5:59AM: Night). Although there was no significant interaction between group and time of death for Cat-S concentration, a general reduction in Cat-S levels was observed in DS-CA subjects. Notably, individuals who died at night exhibited significantly lower Cat-S concentration (time of death x group $F(1,19) = 1.53$, $P = 0.23$; time of death $F(1,19) = 2.40$, $P = 0.14$; group $F(1,19) = 5.55$, $P = 0.029$; followed by Fisher's LSD post-hoc test, **Fig. 3F**).

Lastly, immunoblotting experiments targeting the neo-epitope of aggrecan cleaved by MMPs at the DIPEN terminal (location of cleavage by MMP-2 and MMP-9) in whole grey matter from the vmPFC revealed a trend towards a significant reduction in the digestion of aggrecan core proteins by gelatinases in vmPFC samples from DS-CA individuals ($P = 0.058$, **Fig. 3G-H**).

Discussion

In this study, we sought to explore potential mechanisms underlying the child abuse-associated increase in vmPFC PNNs recently reported by our group (Tanti et al., 2022). We focused mainly on microglial factors, and more specifically on MMP-mediated regulation. Our results indicating a significant downregulation of MMPs, TIMPs and other factors involved in intercellular communication in vmPFC samples from DS-CA compared to CTRL are consistent with our previous finding of increased PNN density.

Examining the molecular landscape through the MMP antibody array highlighted a reduction in MMP-9 in DS-CA compared to CTRL, which was evident in both vmPFC whole grey matter lysate and isolated microglia. Furthermore, the decrease in aggrecan core protein cleavage by MMPs, which was nearly statistically significantly, suggests not only a decline in abundance but also a decrease in enzymatic activity of the MMPs. Interestingly, MMPs are synthesized in a pro-form that remains inactive until proteolytic cleavage. Importantly, this cleavage can be regulated by inflammatory mediators including cytokines, chemokines, free radicals and steroids, or even by other MMPs (Laronha & Caldeira, 2020). We also found reduced TIMPs, specifically microglial TIMP-2, which implies a broader dysregulation of the homeostatic system or a negative feedback loop where decreased MMP activity results in the need for fewer inhibitors. While the current study represents the first postmortem assessment of MMPs in child abuse victims, polymorphism in the MMP-9 gene has previously been suggested to increase susceptibility to depression, although conflicting reports on MMP-9 levels in depressed patients suggest a complex relationship (Beroun et al., 2019; H. Li et al., 2022).

In another set of experiments, we measured the levels of microglial canonical markers implicated in phagocytosis and/or ECM regulation, such as CD68, CX3CR1, IL33R, Cat-S and TREM2. Upon exploring mediators of intercellular communication, particularly through neuronal activation of microglial phagocytosis of ECM components, we observed a strong reduction in the microglial receptors of these signals (CX3CR1 and ILL33R) and no change in microglial activation using CD68 or TREM2 as a proxy. Fractalkine signaling (neural CX3CL1 and microglial CX3CR1 interaction) plays a fundamental role in microglial activity and response to the environment. CX3CR1 deficiency has been shown to impair neuron–microglia communication under chronic

unpredictable stress leading to a lack of responsiveness by microglia (Milior et al., 2016). Furthermore, chemokine receptor CX3CR1 is involved in microglial activation and induction of phagocytotic activity (Müller & Claff, 2022). In a pioneering study by Tansley et al., CX3CR1 knockout (KO) mice subjected to sciatic nerve injury exhibited diminished PNN degradation and reduced lysosomal glycosaminoglycan accumulation within microglia, a stark contrast to the outcomes observed in wild-type mice (Tansley et al., 2022). Reduced levels of CX3CR1 in the vmPFC of DS-CA might underlie the increased number of PNNs reported in these subjects (Tanti et al., 2022).

In a similar vein, IL33 signaling through IL33R is necessary for proper central nervous system formation and functioning (Dwyer et al., 2022). During neurodevelopment, astrocytic release of IL33 plays a crucial role in activating microglia to clear excessive synapses (Vainchtein et al., 2018). Conversely, the expression of neuronal IL33 is experience-dependent, leading to microglial engulfment of ECM in the adult hippocampus (Nguyen et al., 2020). In our study, we found a child abuse-associated downregulation of IL33R, in a brain area exhibiting a child abuse-associated increase in WFL+ PNNs (Tanti et al., 2022). This suggests a diminished signaling cascade between IL33 and IL33R, resulting in attenuated ECM digestion, as observed by Nguyen and colleagues (2020) in neuronal IL33 knock-outs (Nguyen et al., 2020). Interestingly, IL-33 also has the capacity to induce polarization of microglia towards an anti-inflammatory phenotype via its interaction with IL33R (Jia et al., 2023), although the intricacies of this pathway remain only partially defined. Interpreting our findings with this information suggests a plausible diminished anti-inflammatory signaling in our subjects, potentially fostering a tendency towards heightened neuroinflammation—a phenomenon already delineated in the context of depression and ELS

(Rahimian et al., 2022; Rahimian et al., 2021; Reemst et al., 2022). However, this is the first study to examine IL33/IL33R pathways in adults who experienced child abuse, warranting further comprehensive investigations to elucidate these intricate mechanisms.

Another noteworthy enzyme, Cat-S, has been proposed as an ECM regulator influenced by the circadian rhythm (Pantazopoulos et al., 2020). Cat-S secreted from microglia contributes to the diurnal variation in cortical neuron spine density through proteolytic changes of peri-synaptic ECM (Nakanishi, 2020). Both mouse and human brains exhibit diurnal fluctuations of Cat-S expression in microglia that are antiphase to WFL+ PNN densities, with high Cat-S expression being associated with low WFL+ PNN expression. Interestingly, these rhythms are region-specific, as revealed by human thalamic reticular nucleus expressing more WFL+ PNNs at night and fewer during the day, while the amygdala exhibits an inverse pattern (Pantazopoulos et al., 2020). Furthermore, activated Cat-S incubated with mouse brain sections for just 3 hours reduces WFL+ PNNs, while 24 hours eliminates them completely, highlighting microglial Cat-S specific role in PNN degradation (Pantazopoulos et al., 2020). Interestingly Cat-S can promote the generation of soluble CX3CL1 (the CX3CR1 ligand) (Fonović et al., 2013). The lower expression of Cat-S in individuals with a history of child abuse suggests a reduced availability of CX3CL1 for CX3CR1, indicating that child adversity is associated with both lower Cat-S expression and diminished availability of CX3CL1 for CX3CR1.

During development, microglia exhibit heightened activity, playing a crucial role in shaping and refining immature neural circuits through the regulation of neurogenesis, synaptogenesis and synaptic pruning (Crapser et al., 2021; Wright-Jin & Gutmann, 2019). Changes in microglial

function during this developmental period have been shown to impact these processes, influencing behavior. However, the specific impact of early-life adversity on microglia has remained largely unexplored until recently (Bolton et al., 2022; Dayananda et al., 2023; Johnson & Kaffman, 2018). A recent study by the Korosi lab, in collaboration with our group, has shown an enduring effect of early-life stress, induced by limited bedding and nesting, on the microglial transcriptome and function under basal and immune-challenged conditions in mice (Reemst et al., 2022). These effects were found to persist for up to 6 months after exposure to the stress paradigm. In an *in vitro* assay, this study further revealed that microglia exposed to ELS exhibit a reduced capacity for synaptosome phagocytosis in comparison to control microglia (Reemst et al., 2022). Intriguingly, the ELISA findings in the current study also indicate that the phagocytic capacity of microglia is attenuated by having experienced childhood adversity, as evidenced by lower expression of CX3CR1 and IL33R in the DS-CA group. This observation adds a layer of complexity to our understanding of the prolonged impact of early-live adversity on microglial function and its potential implications for synaptic dynamics in the developing brain.

Our study is not without limitations. First, because of limited availability of matched well-characterized samples, the sample size of this study was relatively modest, particularly for experiments isolating microglia from fresh brain samples. This maybe have prevented us from detecting group differences and making sex- or age-specific observations. Second, our study could not distinguish between microglial subpopulations, which respond to distinct cell types (Hashimoto et al., 2023; Ngozi & Bolton, 2022). For instance, there are microglial subpopulations that specifically respond to inhibitory neurons expressing both *Gabbr1* and *Gabbr2*, revealing $GABA_B$ receptiveness (Favuzzi et al., 2021). Furthermore, inhibitory synapse editing in the visual

cortex is mediated by microglial MMP-9 (Hashimoto et al., 2023). Given that PNNs predominantly surround parvalbumin-expressing inhibitory interneurons, it raises a compelling question: is there a specific link between these microglial subpopulations and the regulation of PNNs surrounding parvalbumin-expressing inhibitory neurons in the vmPFC? Despite these limitations, our study provides the first evidence supporting a role for microglia in the child abuse-associated increase in PNNs in the mature vmPFC. Combined with our previous report implicating oligodendrocyte precusor cells in this phenomenon (Tanti et al., 2022), these results further highlight that early-life adversity has a lasting impact on glial cells, with consequences for the neuroplasticity of brain circuitries implicated in cognition and mood.

Author contributions

CB, RR and NM conceived the study. GT participated in the acquisition and clinical characterization of the brain samples. CB, RR, GF and MAD contributed to experiments. BG and NM supervised the study. CB conducted data analysis. CB, RR and NM prepared the manuscript and all other authors contributed and approved of its final version.

Funding

This study was funded by a CIHR Project grant to N.M. R.R. and G.F. received fellowships and C.B. a scholarship from the FRQ-S. The Douglas-Bell Canada Brain Bank is supported in part by platform support grants from the Réseau Québécois sur le Suicide, les Troubles de l'Humeur et les Troubles Associés (FRQ-S), Healthy Brains for Healthy Lives (CFREF), and Brain Canada.

Conflict of interest

The authors declare no conflict of interest.

Figure legends

A

	A	B	C	D	E	F	G	H
1	POS	POS	NEG	NEG	MMP-1	MMP-2	MMP-3	MMP-8
2								
3	MMP-9	MMP-10	MMP-13	TIMP-1	TIMP-2	TIMP-4	NEG	POS
4								

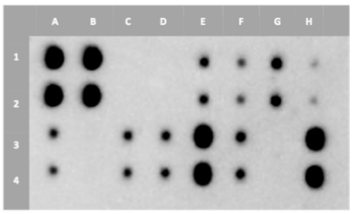

B Gelatinases

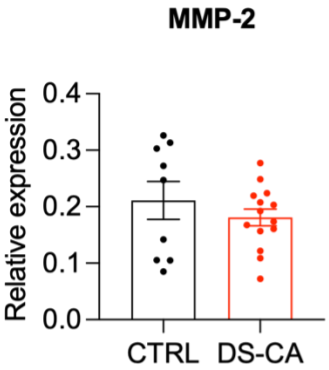

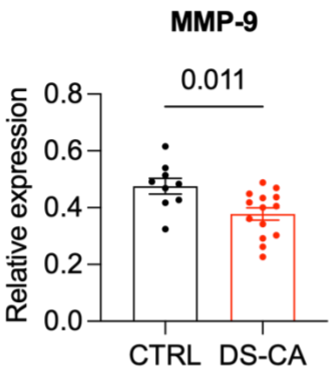

C Stromelysins

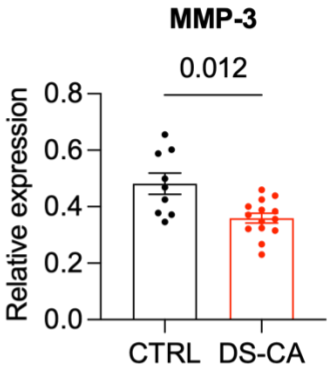

D Collagenases

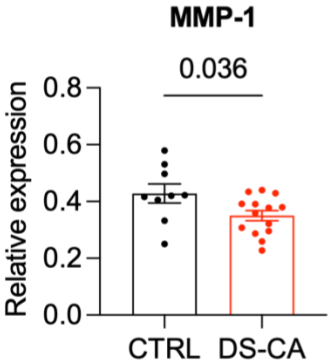

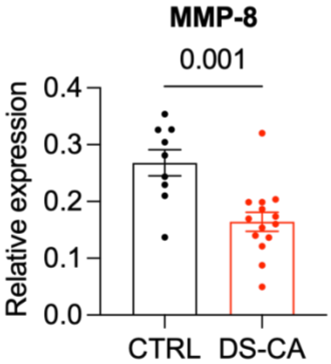

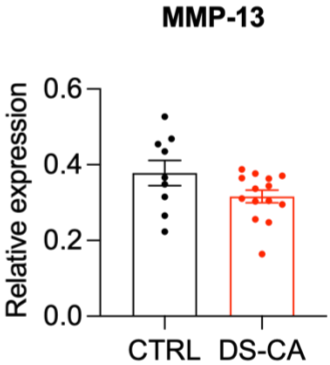

E Endogenous tissue inhibitors

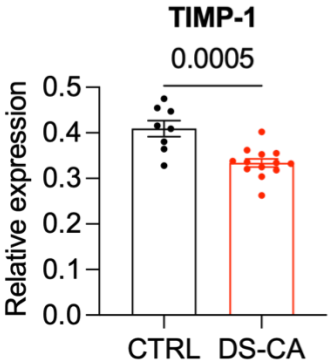

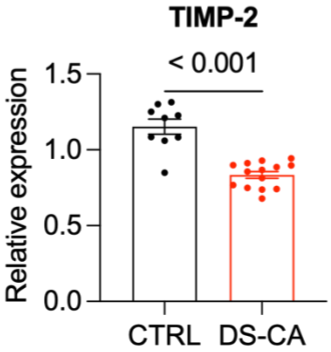

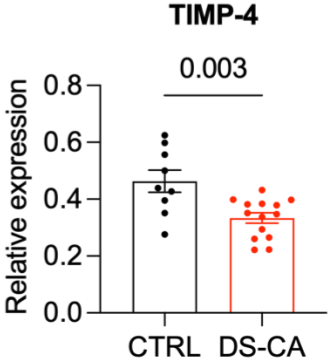

Figure 1: Most of the examined matrix metalloproteinases and their inhibitors are downregulated in vmPFC grey matter from depressed suicides with a history of child abuse compared to matched controls. A Map of the human MMP Array (RayBiotec®) used and a representative blot. Each antibody is spotted in duplicate on the membrane, mean intensity was averaged per antibody as described in the Methods section. **B** MMP-9, **C** MMP-3, **D** MMP-1 and MMP-8 and **E** TIMP-1, -2, -4 are significantly decreased in DS-CA compared to CTRL. POS: positive control, NEG: negative control, MMP: matrix metalloproteinase, TIMP: endogenous tissue inhibitor, CTRL: controls, DS-CA: depressed suicides with a history of child abuse

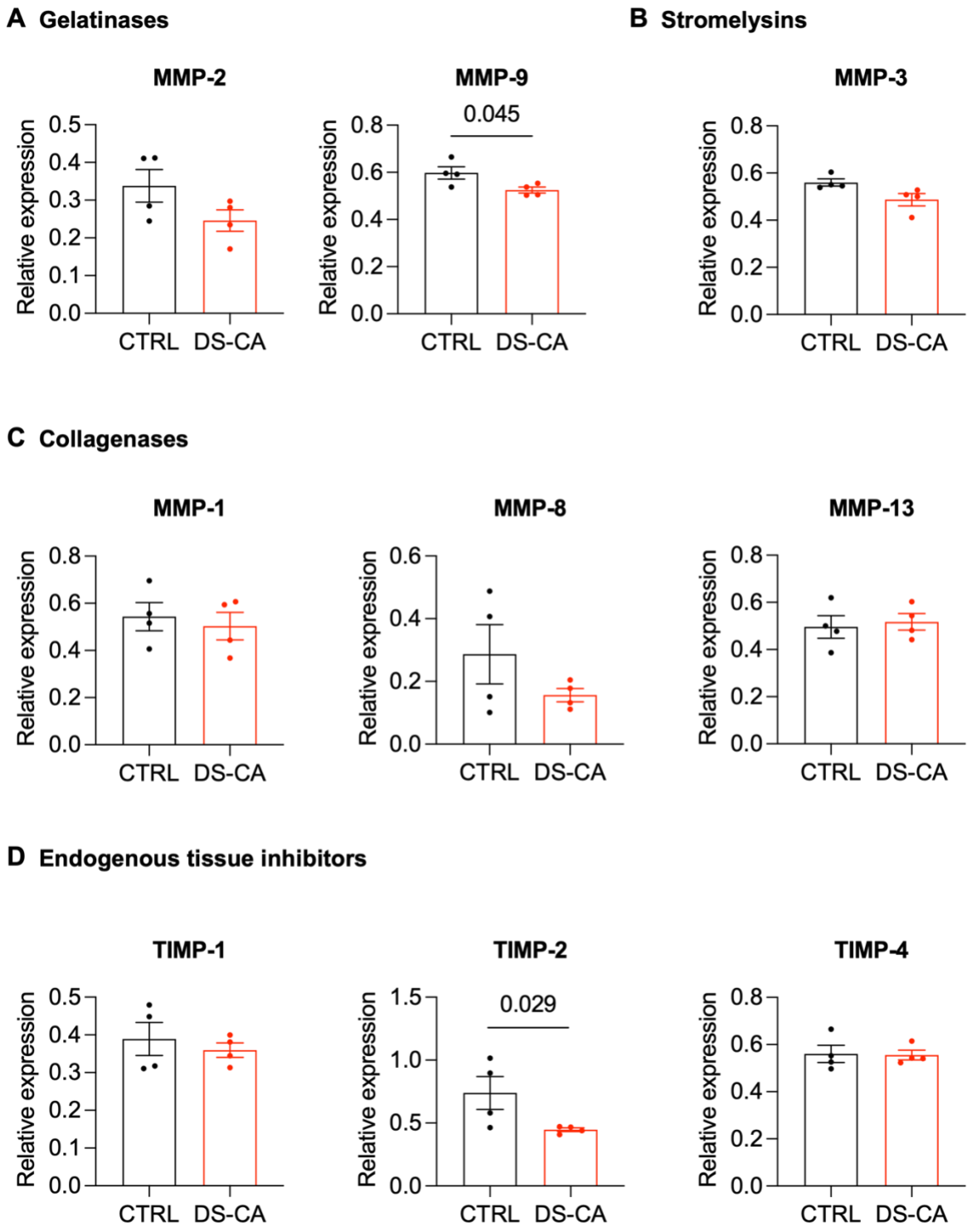

Figure 2: Microglia secrete less MMP-9 and TIMP-2 in vmPFC samples from depressed suicides with a history of child abuse compared to matched controls. A-D Only MMP-9 and inhibitor TIMP-2 are significantly decreased in microglia isolated from the vmPFC of DS-CA.

MMP: matrix metalloproteinase, TIMP: endogenous tissue inhibitor, CTRL: controls, DS-CA: depressed suicide with a history of child abuse.

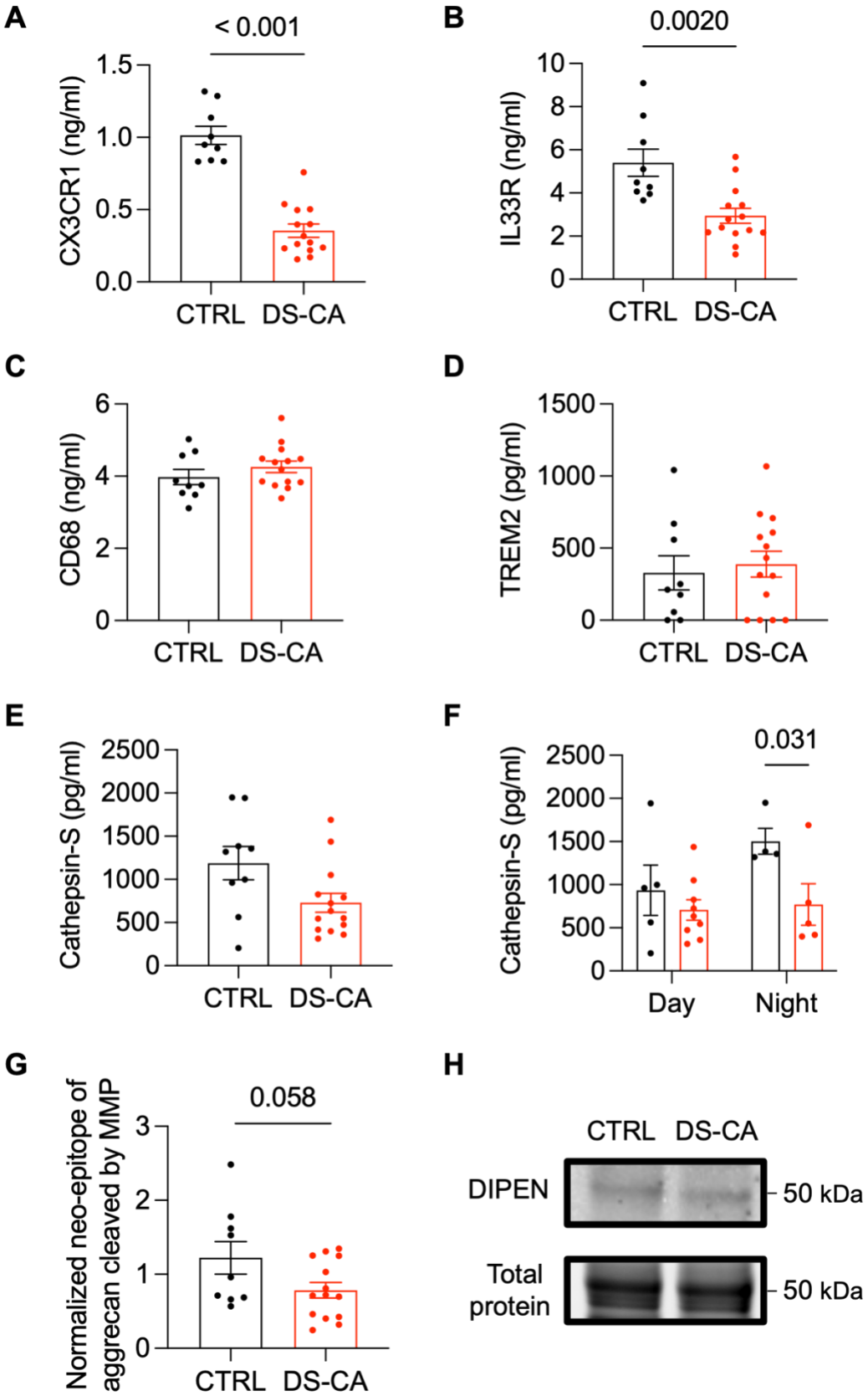
A
< 0.001
CX3CR1 (ng/ml)
1.5
1.0
0.5
0.0
CTRL
DS-CA
B
0.0020
IL33R (ng/ml)
10
8
6
4
2
0
CTRL
DS-CA
C
CD68 (ng/ml)
6
4
2
0
CTRL
DS-CA
D
TREM2 (pg/ml)
1500
1000
500
0
CTRL
DS-CA
E
Cathepsin-S (pg/ml)
2500
2000
1500
1000
500
0
CTRL
DS-CA
F
0.031
Cathepsin-S (pg/ml)
2500
2000
1500
1000
500
0
Day
Night
G
0.058
Normalized neo-epitope of aggrecan cleaved by MMP
3
2
1
0
CTRL
DS-CA
H
CTRL
DS-CA
DIPEN
50 kDa
Total protein
50 kDa

Figure 3: Intercellular communication between neurons and microglia is dampened in vmPFC samples from depressed suicides with a history of child abuse compared to matched controls. **A** CX3CR1 and **B** IL33R are significantly decreased in DS-CA compared to CTRL as investigated by ELISA. **C** CD68 and **D** TREM2 are not associated with changes associated with child abuse. **E-F** Cathepsin-S levels are significantly lower in DS-CA that died at night (between 6:00PM-5:59AM) **G-H** The cleavage of aggrecan core protein in DS-CA by MMPs at the DIPEN terminal is showing a slight reduction compared to CTRL. CX3CR1: CX3C motif chemokine receptor 1, IL33R: interleukin 33 receptor, CD68: cluster of differentiation 68, TREM2: triggering receptor expressed on myeloid cells 2), ELISA: enzyme-linked immunosorbent assay, MMP: matrix metalloproteinase, CTRL: control, DS-CA: depressed suicide with a history of child abuse.

Table 1: Archived frozen brain samples group characteristics			
	CTRL	**DS-CA**	**p-value**
N = 23	9	14	
Axis 1 diagnosis	0	MDD (8); DD-NOS (6)	
Age (years)	51.11 ± 12.72	50.07 ± 12.86	0.85
Sex (M/F)	6/3	10/4	
PMI (hours)	58.59 ± 14.62	57.94 ± 14.89	0.92
Tissue pH	6.17 ± 0.23	6.26 ± 0.29	0.44
Substance dependence	0	Alcohol (1); Cannabis (2)	
Medication prescribed in past three months	Benzodiazepines (1)	Benzodiazepines (1); SNRI (2); SSRI (4); SARI (1); Antipsychotic (2); TCA (2); Opioid (1); Anxiolytic (1); GABA analog (1)	
Data presented as mean ± standard deviation			

Table 2: Fresh brain samples group characteristics			
	CTRL	**DS-CA**	**p-value**
N = 8	4	4	
Axis 1 diagnosis	0	MDD (2); DD-NOS (2)	
Age (years)	53.25 ± 12.87	55.5 ± 6.45	0.77
Sex (M/F)	2/2	2/2	
PMI (hours)	51.52 ± 7.37	49.63 ± 2.50	0.66
Tissue pH	6.45 ± 0.33	5.89 ± 0.25	0.23
Substance dependence	0	0	
Medication prescribed in past three months	Benzodiazepines (1)	SSRI (2); Anxiolytic (1); Benzodiazepine (1)	
Data presented as mean ± standard deviation			

References

A. Dumais, B.Sc. ,, A.D. Lesage, M.D., M.Phil. ,, M. Alda, M.D. ,, G. Rouleau, M.D., Ph.D. ,, M. Dumont, R.N. ,, N. Chawky, M.Ps. ,, M. Roy, M.D. ,, J.J. Mann, M.D. ,, C. Benkelfat, M.D. , and, & Gustavo Turecki, M.D., Ph.D. (2005). Risk Factors for Suicide Completion in Major Depression: A Case-Control Study of Impulsive and Aggressive Behaviors in Men. *American Journal of Psychiatry*, *162*(11), 2116-2124. https://doi.org/10.1176/appi.ajp.162.11.2116

Alaiyed, S., Bozzelli, P. L., Caccavano, A., Wu, J. Y., & Conant, K. (2019). Venlafaxine stimulates PNN proteolysis and MMP-9-dependent enhancement of gamma power; relevance to antidepressant efficacy. *J Neurochem*, *148*(6), 810-821. https://doi.org/10.1111/jnc.14671

Arreola, M. A., Soni, N., Crapser, J. D., Hohsfield, L. A., Elmore, M. R. P., Matheos, D. P., Wood, M. A., Swarup, V., Mortazavi, A., & Green, K. N. (2021). Microglial dyshomeostasis drives perineuronal net and synaptic loss in a CSF1R+/- mouse model of ALSP, which can be rescued via CSF1R inhibitors. *Science Advances*, *7*(35), eabg1601. https://doi.org/doi:10.1126/sciadv.abg1601

Beroun, A., Mitra, S., Michaluk, P., Pijet, B., Stefaniuk, M., & Kaczmarek, L. (2019). MMPs in learning and memory and neuropsychiatric disorders. *Cell Mol Life Sci*, *76*(16), 3207-3228. https://doi.org/10.1007/s00018-019-03180-8

Bifulco, A., Brown, G. W., & Harris, T. O. (1994). Childhood Experience of Care and Abuse (CECA): a retrospective interview measure. *J Child Psychol Psychiatry*, *35*(8), 1419-1435. https://doi.org/10.1111/j.1469-7610.1994.tb01284.x

Bitanihirwe, B. K. Y., & Woo, T.-U. W. (2020). A conceptualized model linking matrix metalloproteinase-9 to schizophrenia pathogenesis. *Schizophrenia Research*, *218*, 28-35. https://doi.org/10.1016/j.schres.2019.12.015

Bolton, J. L., Short, A. K., Othy, S., Kooiker, C. L., Shao, M., Gunn, B. G., Beck, J., Bai, X., Law, S. M., & Savage, J. C. (2022). Early stress-induced impaired microglial pruning of excitatory synapses on immature CRH-expressing neurons provokes aberrant adult stress responses. *Cell reports*, *38*(13).

Boutej, H., Rahimian, R., Thammisetty, S. S., Béland, L. C., Lalancette-Hébert, M., & Kriz, J. (2017). Diverging mRNA and Protein Networks in Activated Microglia Reveal SRSF3 Suppresses Translation of Highly Upregulated Innate Immune Transcripts. *Cell Rep*, *21*(11), 3220-3233. https://doi.org/10.1016/j.celrep.2017.11.058

Catale, C., Gironda, S., Lo Iacono, L., & Carola, V. (2020). Microglial Function in the Effects of Early-Life Stress on Brain and Behavioral Development. *J Clin Med*, *9*(2). https://doi.org/10.3390/jcm9020468

Crapser, J. D., Arreola, M. A., Tsourmas, K. I., & Green, K. N. (2021). Microglia as hackers of the matrix: sculpting synapses and the extracellular space. *Cell Mol Immunol*, *18*(11), 2472-2488. https://doi.org/10.1038/s41423-021-00751-3

Crapser, J. D., Ochaba, J., Soni, N., Reidling, J. C., Thompson, L. M., & Green, K. N. (2020). Microglial depletion prevents extracellular matrix changes and striatal volume reduction in a model of Huntington's disease. *Brain*, *143*(1), 266-288. https://doi.org/10.1093/brain/awz363

Crapser, J. D., Spangenberg, E. E., Barahona, R. A., Arreola, M. A., Hohsfield, L. A., & Green, K. N. (2020). Microglia facilitate loss of perineuronal nets in the Alzheimer's disease brain. *EBioMedicine*, *58*, 102919. https://doi.org/10.1016/j.ebiom.2020.102919

Dayananda, K. K., Ahmed, S., Wang, D., Polis, B., Islam, R., & Kaffman, A. (2023). Early life stress impairs synaptic pruning in the developing hippocampus. *Brain Behav Immun*, *107*, 16-31. https://doi.org/10.1016/j.bbi.2022.09.014

Dwyer, G. K., D'Cruz, L. M., & Turnquist, H. R. (2022). Emerging Functions of IL-33 in Homeostasis and Immunity. *Annu Rev Immunol*, *40*, 15-43. https://doi.org/10.1146/annurev-immunol-101320-124243

Dzyubenko, E., & Hermann, D. M. (2023). Role of glia and extracellular matrix in controlling neuroplasticity in the central nervous system. *Seminars in Immunopathology*, *45*(3), 377-387. https://doi.org/10.1007/s00281-023-00989-1

Favuzzi, E., Huang, S., Saldi, G. A., Binan, L., Ibrahim, L. A., Fernández-Otero, M., Cao, Y., Zeine, A., Sefah, A., Zheng, K., Xu, Q., Khlestova, E., Farhi, S. L., Bonneau, R., Datta, S. R., Stevens, B., & Fishell, G. (2021). GABA-receptive microglia selectively sculpt developing inhibitory circuits. *Cell*, *184*(15), 4048-4063.e4032. https://doi.org/https://doi.org/10.1016/j.cell.2021.06.018

Fonović, U. P., Jevnikar, Z., & Kos, J. (2013). Cathepsin S generates soluble CX3CL1 (fractalkine) in vascular smooth muscle cells. *Biol Chem*, *394*(10), 1349-1352. https://doi.org/10.1515/hsz-2013-0189

Hashimoto, A., Kawamura, N., Tarusawa, E., Takeda, I., Aoyama, Y., Ohno, N., Inoue, M., Kagamiuchi, M., Kato, D., Matsumoto, M., Hasegawa, Y., Nabekura, J., Schaefer, A., Moorhouse, A. J., Yagi, T., & Wake, H. (2023). Microglia enable cross-modal plasticity

by removing inhibitory synapses. *Cell Rep*, *42*(5), 112383. https://doi.org/10.1016/j.celrep.2023.112383

Hiser, J., & Koenigs, M. (2018). The Multifaceted Role of the Ventromedial Prefrontal Cortex in Emotion, Decision Making, Social Cognition, and Psychopathology. *Biol Psychiatry*, *83*(8), 638-647. https://doi.org/10.1016/j.biopsych.2017.10.030

Javanmehr, N., Saleki, K., Alijanizadeh, P., & Rezaei, N. (2022). Microglia dynamics in aging-related neurobehavioral and neuroinflammatory diseases. *Journal of Neuroinflammation*, *19*(1), 273. https://doi.org/10.1186/s12974-022-02637-1

Jia, Z., Guo, M., Ge, X., Chen, F., & Lei, P. (2023). IL-33/ST2 Axis: A Potential Therapeutic Target in Neurodegenerative Diseases. *Biomolecules*, *13*(10), 1494. https://www.mdpi.com/2218-273X/13/10/1494

Johnson, F. K., & Kaffman, A. (2018). Early life stress perturbs the function of microglia in the developing rodent brain: New insights and future challenges. *Brain Behav Immun*, *69*, 18-27. https://doi.org/10.1016/j.bbi.2017.06.008

Juergen Mai, M. M., George Paxinos. (2016). *Atlas of the Human Brain. 4th Ed*. Elseiver.

Könnecke, H., & Bechmann, I. (2013). The role of microglia and matrix metalloproteinases involvement in neuroinflammation and gliomas. *Clin Dev Immunol*, *2013*, 914104. https://doi.org/10.1155/2013/914104

Laronha, H., & Caldeira, J. (2020). Structure and Function of Human Matrix Metalloproteinases. *Cells*, *9*(5). https://doi.org/10.3390/cells9051076

Li, B., Yang, W., Ge, T., Wang, Y., & Cui, R. (2022). Stress induced microglial activation contributes to depression. *Pharmacol Res*, *179*, 106145. https://doi.org/10.1016/j.phrs.2022.106145

Li, H., Sheng, Z., Khan, S., Zhang, R., Liu, Y., Zhang, Y., Yong, V. W., & Xue, M. (2022). Matrix Metalloproteinase-9 as an Important Contributor to the Pathophysiology of Depression. *Front Neurol*, *13*, 861843. https://doi.org/10.3389/fneur.2022.861843

Milior, G., Lecours, C., Samson, L., Bisht, K., Poggini, S., Pagani, F., Deflorio, C., Lauro, C., Alboni, S., Limatola, C., Branchi, I., Tremblay, M. E., & Maggi, L. (2016). Fractalkine receptor deficiency impairs microglial and neuronal responsiveness to chronic stress. *Brain Behav Immun*, *55*, 114-125. https://doi.org/10.1016/j.bbi.2015.07.024

Monnier, P. P., Sierra, A., Schwab, J. M., Henke-Fahle, S., & Mueller, B. K. (2003). The Rho/ROCK pathway mediates neurite growth-inhibitory activity associated with the chondroitin sulfate proteoglycans of the CNS glial scar. *Mol Cell Neurosci*, *22*(3), 319-330. https://doi.org/10.1016/s1044-7431(02)00035-0

Müller, C. E., & Claff, T. (2022). Activated microglia nibbling glycosaminoglycans from spinal cord perineural nets: a new mechanism for neuropathic pain. *Signal Transduct Target Ther*, *7*(1), 333. https://doi.org/10.1038/s41392-022-01162-0

Nakanishi, H. (2020). Cathepsin regulation on microglial function. *Biochim Biophys Acta Proteins Proteom*, *1868*(9), 140465. https://doi.org/10.1016/j.bbapap.2020.140465

Ngozi, Z., & Bolton, J. L. (2022). Microglia Don't Treat All Neurons the Same: The Importance of Neuronal Subtype in Microglia-Neuron Interactions in the Developing Hypothalamus [Perspective]. *Frontiers in Cellular Neuroscience*, *16*. https://www.frontiersin.org/articles/10.3389/fncel.2022.867217

Nguyen, P. T., Dorman, L. C., Pan, S., Vainchtein, I. D., Han, R. T., Nakao-Inoue, H., Taloma, S. E., Barron, J. J., Molofsky, A. B., Kheirbek, M. A., & Molofsky, A. V. (2020).

Microglial Remodeling of the Extracellular Matrix Promotes Synapse Plasticity. *Cell*, *182*(2), 388-403.e315. https://doi.org/10.1016/j.cell.2020.05.050

Pantazopoulos, H., Gisabella, B., Rexrode, L., Benefield, D., Yildiz, E., Seltzer, P., Valeri, J., Chelini, G., Reich, A., Ardelt, M., & Berretta, S. (2020). Circadian Rhythms of Perineuronal Net Composition. *eNeuro*, *7*(4). https://doi.org/10.1523/eneuro.0034-19.2020

Pearson, C. S., Mencio, C. P., Barber, A. C., Martin, K. R., & Geller, H. M. (2018). Identification of a critical sulfation in chondroitin that inhibits axonal regeneration. *eLife*, *7*. https://doi.org/10.7554/eLife.37139

Rahimian, R., Belliveau, C., Chen, R., & Mechawar, N. (2022). Microglial Inflammatory-Metabolic Pathways and Their Potential Therapeutic Implication in Major Depressive Disorder. *Front Psychiatry*, *13*, 871997. https://doi.org/10.3389/fpsyt.2022.871997

Rahimian, R., Guruswamy, R., Boutej, H., Cordeau, P., Jr., Weng, Y. C., & Kriz, J. (2024). Targeting SRSF3 restores immune mRNA translation in microglia/macrophages following cerebral ischemia. *Mol Ther*, *32*(3), 783-799. https://doi.org/10.1016/j.ymthe.2024.01.004

Rahimian, R., Wakid, M., O'Leary, L. A., & Mechawar, N. (2021). The emerging tale of microglia in psychiatric disorders. *Neurosci Biobehav Rev*, *131*, 1-29. https://doi.org/10.1016/j.neubiorev.2021.09.023

Reemst, K., Kracht, L., Kotah, J. M., Rahimian, R., van Irsen, A. A. S., Congrains Sotomayor, G., Verboon, L. N., Brouwer, N., Simard, S., Turecki, G., Mechawar, N., Kooistra, S. M., Eggen, B. J. L., & Korosi, A. (2022). Early-life stress lastingly impacts microglial

transcriptome and function under basal and immune-challenged conditions. *Translational Psychiatry*, *12*(1), 507. https://doi.org/10.1038/s41398-022-02265-6

Schramm, E., & Waisman, A. (2022). Microglia as Central Protagonists in the Chronic Stress Response. *Neurol Neuroimmunol Neuroinflamm*, *9*(6). https://doi.org/10.1212/nxi.0000000000200023

Sigal, Y. M., Bae, H., Bogart, L. J., Hensch, T. K., & Zhuang, X. (2019). Structural maturation of cortical perineuronal nets and their perforating synapses revealed by superresolution imaging. *Proc Natl Acad Sci U S A*, *116*(14), 7071-7076. https://doi.org/10.1073/pnas.1817222116

Sun, J., Wang, X., Sun, R., Xiao, X., Wang, Y., Peng, Y., & Gao, Y. (2023). Microglia shape AgRP neuron postnatal development via regulating perineuronal net plasticity. *Molecular Psychiatry*. https://doi.org/10.1038/s41380-023-02326-2

Tansley, S., Gu, N., Guzmán, A. U., Cai, W., Wong, C., Lister, K. C., Muñoz-Pino, E., Yousefpour, N., Roome, R. B., Heal, J., Wu, N., Castonguay, A., Lean, G., Muir, E. M., Kania, A., Prager-Khoutorsky, M., Zhang, J., Gkogkas, C. G., Fawcett, J. W., . . . Khoutorsky, A. (2022). Microglia-mediated degradation of perineuronal nets promotes pain. *Science*, *377*(6601), 80-86. https://doi.org/doi:10.1126/science.abl6773

Tanti, A., Belliveau, C., Nagy, C., Maitra, M., Denux, F., Perlman, K., Chen, F., Mpai, R., Canonne, C., Théberge, S., McFarquhar, A., Davoli, M. A., Belzung, C., Turecki, G., & Mechawar, N. (2022). Child abuse associates with increased recruitment of perineuronal nets in the ventromedial prefrontal cortex: a possible implication of oligodendrocyte progenitor cells. *Molecular Psychiatry*, *27*(3), 1552-1561. https://doi.org/10.1038/s41380-021-01372-y

Teicher, M. H., Samson, J. A., Anderson, C. M., & Ohashi, K. (2016). The effects of childhood maltreatment on brain structure, function and connectivity. *Nat Rev Neurosci*, *17*(10), 652-666. https://doi.org/10.1038/nrn.2016.111

Torres-Platas, S. G., Cruceanu, C., Chen, G. G., Turecki, G., & Mechawar, N. (2014). Evidence for increased microglial priming and macrophage recruitment in the dorsal anterior cingulate white matter of depressed suicides. *Brain Behav Immun*, *42*, 50-59. https://doi.org/10.1016/j.bbi.2014.05.007

Troubat, R., Barone, P., Leman, S., Desmidt, T., Cressant, A., Atanasova, B., Brizard, B., El Hage, W., Surget, A., Belzung, C., & Camus, V. (2021). Neuroinflammation and depression: A review. *Eur J Neurosci*, *53*(1), 151-171. https://doi.org/10.1111/ejn.14720

Tsien, R. Y. (2013). Very long-term memories may be stored in the pattern of holes in the perineuronal net. *Proc Natl Acad Sci U S A*, *110*(30), 12456-12461. https://doi.org/10.1073/pnas.1310158110

Vainchtein, I. D., Chin, G., Cho, F. S., Kelley, K. W., Miller, J. G., Chien, E. C., Liddelow, S. A., Nguyen, P. T., Nakao-Inoue, H., & Dorman, L. C. (2018). Astrocyte-derived interleukin-33 promotes microglial synapse engulfment and neural circuit development. *Science*, *359*(6381), 1269-1273.

Venturino, A., Schulz, R., De Jesús-Cortés, H., Maes, M. E., Nagy, B., Reilly-Andújar, F., Colombo, G., Cubero, R. J. A., Schoot Uiterkamp, F. E., Bear, M. F., & Siegert, S. (2021). Microglia enable mature perineuronal nets disassembly upon anesthetic ketamine exposure or 60-Hz light entrainment in the healthy brain. *Cell Rep*, *36*(1), 109313. https://doi.org/10.1016/j.celrep.2021.109313

Wen, T. H., Afroz, S., Reinhard, S. M., Palacios, A. R., Tapia, K., Binder, D. K., Razak, K. A., & Ethell, I. M. (2017). Genetic Reduction of Matrix Metalloproteinase-9 Promotes Formation of Perineuronal Nets Around Parvalbumin-Expressing Interneurons and Normalizes Auditory Cortex Responses in Developing Fmr1 Knock-Out Mice. *Cerebral Cortex*, *28*(11), 3951-3964. https://doi.org/10.1093/cercor/bhx258

Wright-Jin, E. C., & Gutmann, D. H. (2019). Microglia as Dynamic Cellular Mediators of Brain Function. *Trends in Molecular Medicine*, *25*(11), 967-979. https://doi.org/https://doi.org/10.1016/j.molmed.2019.08.013